COMFORT ANALYSIS OF VEHICLE DRIVER'S SEAT THROUGH SIMULATION OF THE SITTING PROCESS

Ile Mircheski, Tatjana Kandikjan, Sofija Sidorenko

In this paper, a method for ergonomic analysis of the seating comfort in the driver's seat for passenger vehicles is presented in two phases. In the first phase, the comfort seating postures of the driver are analyzed considering the comfort angles for the placement of human body and the necessary space for foot controls in vehicles, as well as the ranges of adjustments of the driver's seat and steering wheel. According to the determined comfort postures, the seat-human body virtual system is modeled. In the second phase, virtual testing of the seating comfort is performed with two different body sizes for 50th and 80th percentiles of virtual mannequins. The results can be used further to improve the arrangement of the basic comfort components for the driver's seat in vehicles. Virtual solid model of driver's body and driver's seat was created, especially for analysis of the pressure distribution on the contact surface of the virtual human body and the seat cushion foam. Virtual testing was performed using software package ABAQUS, simulating processes with finite element analysis method (FEA). The testing includes variation of the spatial mechanical properties of polyurethane foam and variation of the male body sizes for 50th and 80th percentiles. The results from the virtual testing were verified experimentally using pressure distribution mapping sensors. Using the virtual testing system for seating comfort, design changes of the seat can be introduced and verified.

Keywords: comfort angles, driver's seat, ergonomics, pressure distribution, virtual human model, virtual mannequin

Analiza udobnosti vozačeva sjedala simulacijom postupka sjedanja

Izvorni znanstveni članak

U ovom se radu u dvije faze predstavlja metoda za ergonomsku analizu udobnosti sjedenja u sjedalu vozača putničkog vozila. U prvoj fazi se udobnost sjedećih položaja vozača analizira razmatrajući kutove pod kojima će ljudsko tijelo biti ugodno smješteno te prostor potreban za nožne komande u vozilu kao i područja za podešavanje sjedala i volana. Prema određenim udobnim položajima modelira se virtualni sustav sjedalo-ljudsko tijelo. U drugoj fazi se obavlja virtualno provjeravanje udobnosti sjedenja koristeći dvije različite dimenzije tijela virtualnih lutaka od 50 i 70 persentila. Rezultati se mogu dalje koristiti za poboljšanje rasporeda osnovnih komponenti koje će doprinijeti udobnosti vozačeva sjedala. Izrađen je virtualni model tijela i sjedala vozača, naročito za analizu raspodjele pritiska na površini kontakta virtualnog ljudskog tijela i pjenaste površine sjedala. Za virtualno ispitivanje se koristio programski paket ABAQUS, koji je simulirao postupke metodom analize konačnih elemenata (FEM). Ispitivanje uključuje variranje prostornih mehaničkih svojstava poliuretanske pjene i variranje dimenzija ljudskog muškog tijela za grupe od 50 i 80 percentila. Rezultati virtualnog ispitivanja su eksperimentalno provjereni primjenom senzora za ucrtavanje distribucije pritiska. Upotrebom virtualnog sustava ispitivanja udobnosti sjedenja mogu se uvesti i provjeriti promjene u dizajniranju sjedala.

Ključne riječi: ergonomija, raspodjela pritiska, ugodni kutovi, virtualni ljudski model, virtualna lutka, vozačevo sjedalo

1 Introduction

The choice of a passenger automobile depends on a variety of factors, such as the vehicle type, brand, trend, security, its performance, interior space, interior design, additional equipment offered, etc. The seat comfort is a very important issue for the drivers. Long time driving usually results in manifestation of low back pain or other musculoskeletal disorders, caused by the discomfort of the seats. Accordingly, the expectations of customers regarding the seat comfort are continuously increasing [1, 2]. The manufacturers of seats for passenger automobiles have to respond to market requirements fast and appropriately and offer seats with higher quality and comfort.

The manufacturers of automobile seats usually make prototypes for testing the comfort in order to achieve the desired results. Testing with prototypes is an expensive and time consuming process [3]. Application of contemporary software products for virtual modeling of vehicle structure, as well as software products for simulation of processes and system behavior, reduces the time for testing of the new vehicle. Contemporary testing of new vehicles starts with virtual testing of virtual models, using virtual humans. The errors and inconveniences are reduced in the early phase. As a consequence, time and price for testing of new or improved vehicles are reduced. The final tests are applied on real models - prototypes.

In the first phase of our research the basic components of the automobile's driver comfort were determined: angles for placement of the human body and the necessary space for the foot controls, as well as the ranges of adjustments of the driver's seat and the steering wheel. In the second phase of our research we determined the influence that the variation of the spatial mechanical properties of the polyurethane foam, such as thickness and density, as well as the shape of the contact surface between the driver the and seat, have upon the seating comfort of the automobile's driver.

2 Determination towards the comfort seating and handling conditions for the driver

The sitting positions of the driver and other passengers, the arrangement of all handling devices and controls, as well as the application of all safety regulations and legislation, are important initial points for the overall dimensioning of the vehicle. The process of design starts with the definition of the user population and by obtaining the human body data.

In order to obtain comfort posture for the drivers of different sizes, many components of the vehicle have to be adjustable. Contemporary vehicles are equipped with

adjustable seats, adjustable steering wheel, adjustable mirrors, etc.

The first part of our research was committed to the definition of the best position of the seat and all handling devices in the vehicle. We started with adoption of the comfort criteria and definition of four different testing conditions with different initial fixed points: fixed eye point, fixed hip point, fixed hand point and fixed heel point.

2.1 Adoption of the comfort criteria

The range of the seat and steering wheel adjustments is closely dependent on the body sizes of the smallest and biggest representative of the selected user population. The analyses were applied to two extreme human sizes: 5th percentile woman and 95th percentile man.

In the case of driver's work position the workspace envelope depends on the position of the driver's body. Several functional measurements are very important parameters in the vehicle: the angles of the elbow joint, shoulder joint, hip joint, knee joint, ankle joint and torso orientation (Fig. 1).
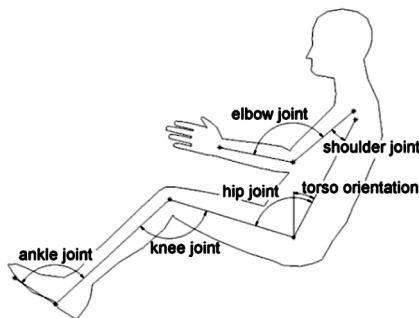

Figure 1 Parameters of driver's work position

Table 1 Adopted comfortable angles for the driver's seating posture

Torso orientation	27°
Angle of shoulder joint	22°
Angle of elbow joint	127°
Angle of hip joint	99°
Angle of knee joint	119°
Angle of ankle joint	103

In order to obtain driving comfort, the driver's seating posture must always be in the comfortable range [3]. For the last few years many researchers have offered their recommendations as regards the ranges of comfortable angles [4]. However, there are big differences in their viewpoints concerning the comfort angles. Some of them recommend discrete comfort angles, and the others opt for ranges of comfort. Given the fact that RAMSIS software [5] is specialized in ergonomics in vehicles we adopted the recommended discrete comfort angles included in the RAMSIS data bases (Tab. 1).

2.2 Examination of the proposed testing concepts

Virtual mannequins of two extreme anthropometric sizes with adopted comfortable posture were examined in four different testing conditions with different initial fixed points: fixed eye point, fixed hip point, fixed hand point and fixed heel point. The results of the testing were the

ranges of necessary horizontal and vertical adjustments of the vehicle's components in order to accommodate drivers of different human sizes.
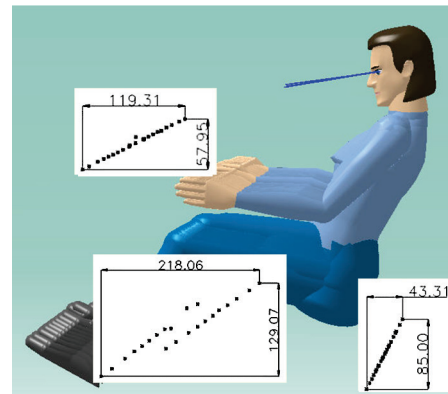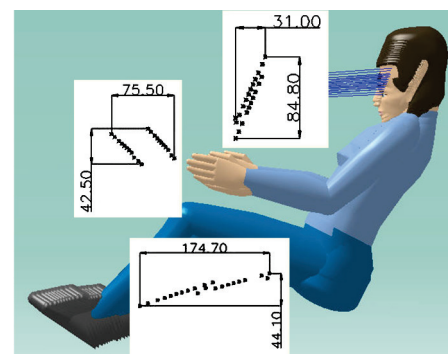

Figure 2 Concept with fixed eye point

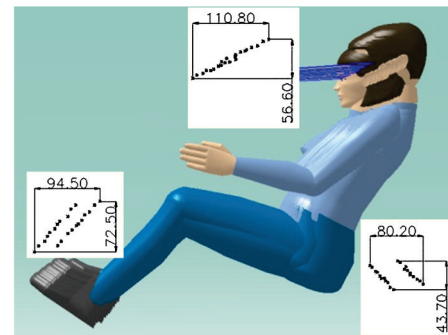**Figure 3** Concept with fixed hip point
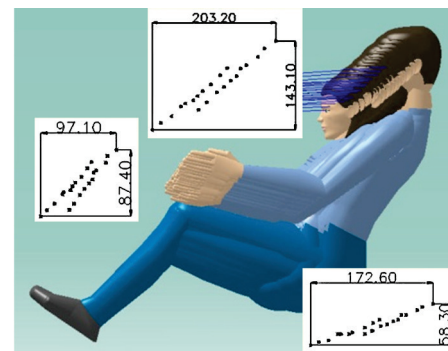

Figure 4 Concept with fixed hand point

Figure 5 Concept with fixed heel point

The concept of fixed eye point for all anthropometric sizes requires the following adjustments (Fig. 2):

• Adjustment of the seat in the horizontal range of 43 mm and vertical range of 85 mm;

- Adjustment of the steering wheel in the horizontal range of 119 mm and vertical range of 58 mm;
- Adjustments of the foot pedals in the horizontal range of 218 mm and in the vertical range of 129 mm.

The driver's seat has to be fixed in the vehicle in the concept of fixed hip point (Fig. 3). This concept for all anthropometric sizes requires the following adjustments:

- Adjustments of the steering wheel: horizontal adjustment of 75 mm and vertical adjustment of 425 mm;
- Adjustments of the foot pedal: horizontal adjustment of 175 mm and vertical adjustment of 44 mm;
- Because of the fixed seat, the eye position could not be positioned on the recommended height: missing horizontal adjustment of 31 mm and vertical adjustment of 85 mm.

The steering wheel has to be fixed in the vehicle in the concept of fixed hand point (Fig. 4). This concept for all anthropometric sizes requires the following adjustments:

- Adjustments of the seat: horizontal adjustment of 80 mm and vertical adjustment of 44 mm;
- Adjustments of the foot pedal: horizontal adjustment of 94 mm and vertical adjustment of 72 mm;
- Because of the fixed steering wheel, the eye point could not be positioned on the recommended height, but it could be neglected because the difference is only 57 mm.

The concept with fixed heel point proposes fixed foot controls (Fig. 5). This concept for all anthropometric sizes requires the following adjustments:

- Adjustment of the seat: horizontal adjustment of 173 mm and vertical adjustment of 58 mm;
- Adjustments of the steering wheel: horizontal adjustment of 97 mm and vertical adjustment of 87 mm;
- Because of the fixed foot controls, the eye point could not be positioned on the recommended height. The difference of 143 mm could not be neglected.

The concept with fixed heel point was accepted as a concept with the best balance between function and driver's comfort.

2.3 Improvement of the selected concept

In order to ensure perfect visibility on the road the eye points of all of the anthropometric sizes have to be placed on or over the line that touches the front profile of the car's shell. The visual line can be defined as a tangent line over the front profile of the car's shell that begins in the eye point of a 95th percentile man. The anthropometric size of the 95th percentile man has the best view as a result of his highest eye position in comparison with other anthropometric sizes.

In order to obtain a good driving comfort the positioning of the pedals for foot controls has to be in accordance with the comfort knee angle. Several

situations of different leg positions, as a result of different pressing forces applied on the pedals were also examined.

The first examined situation was: the right foot in pressing position on the acceleration pedal and the left foot in relaxing position. The results were: comfort positions of two legs and no problems with the visual control (Fig. 6). The problem appeared in the case of clutch pressing: the angle in the left knee was 180°, not comfortable (Fig. 7).
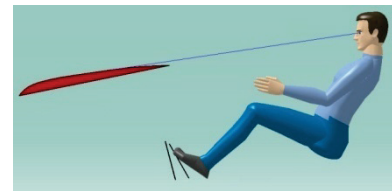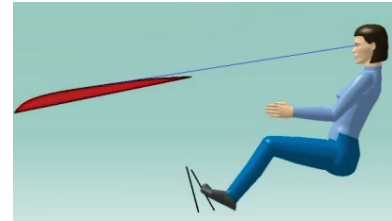

Figure 6 The first examined situation

Figure 7 The problem with clutch pressing

The second examined situation was: the right foot in pressing position on the acceleration pedal and the left foot in pressing position on the clutch pedal.
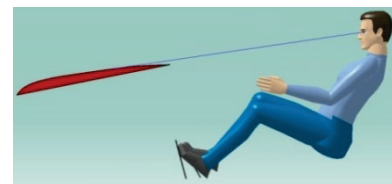

Figure 8 The second examined situation

Both of the models are not acceptable for the final concept: the first one is too far from the pedals, the other one is too close to the pedals. In the first case the left leg is too extended – the knee angle is 180°, in the second

case the right knee angle is 90°. The final decision about the positioning of the pedals was obtained as a result of taking into consideration the importance of the right foot control. Because of the long duration of the pressing position of the right leg on the acceleration pedal, the comfort angle of the right leg in pressing position has to be the initial point.

The left leg is used temporarily for pressing the clutch pedal and it is not necessary to obtain comfort angle. After the examination of two extreme anthropometric sizes, the obtained knee angle for the left pedal was 150° as an acceptable solution.
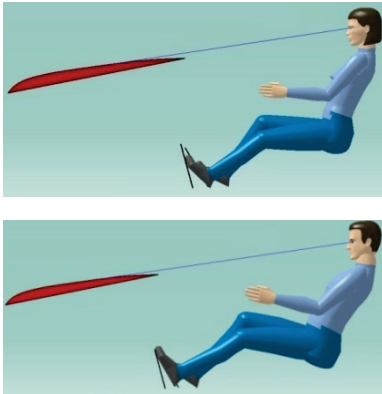

Figure 9 Final concept

Finally, the concept with fixed heel point was accepted with initial comfort angle for the right leg. According to the fact that the determined adjustable ranges for the seat and for the steering wheel obtain perfect vision control for all anthropometric sizes, all of the ergonomic criteria for the accepted concept were fulfilled.

3 Virtual model of human bones and muscles

Geometric data of virtual models of human are taken from the data base of the software module Human Builder in Catia [4, 5, 6]. The virtual human model is composed of two parts, muscle tissue and skeleton. The human skin is not considered in the analysis because it is geometrically very complicated and has small impact on the results of the pressure distribution analysis [7]. The geometry of the skeleton is simplified with the aim to reduce the time needed for calculation of the numerical model with FEA, but the model should not be oversimplified because it will influence the validity of the received values from pressure distribution. Pelvis, femurs and simplified model of skeleton from virtual model of the human are shown in Fig.10. The FEA model for numerical calculation is represented with the meshed model of the human with the characteristics of muscles tissue and bones. The mesh is created with tetrahedron elements, which are suitable for complicated geometric models.

The mesh of human muscle tissue is composed of smaller finite elements than the mesh of simplified model of human skeleton (Fig. 11). The human skeleton is not the goal of this analysis. The goal of the analysis is the human muscle tissue where the real contact with the seat occurs, and from where the values for pressure distribution are read.
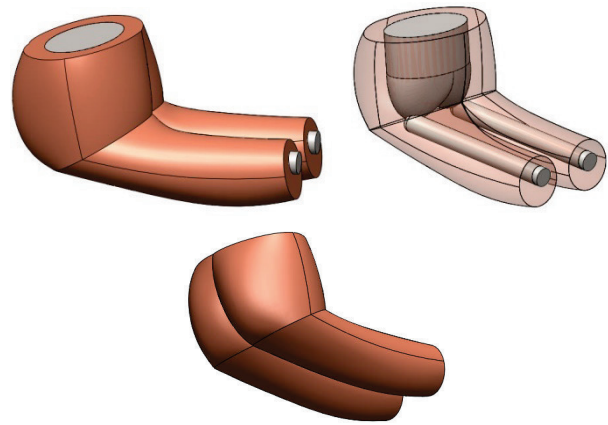

Figure 10 Geometrical representation of part of virtual model of human – pelvis, femurs and simplified muscule tissue

For human bone structures, the skeleton is assumed to be a rigid body. The human skeleton is a rigid body because the bones are not being deformed when the human body is in the seating position.

Figure 11 The FEA mesh model of the seating human

A few of the authors who worked with virtual testing of human muscle tissue are (A. Siefert, S. Pankoke, H. P. Wolfel [8]; and Verver, M. [9]). The authors give different kinds of definition of the human muscle tissue. Verver, M [10] in her doctoral dissertation describes the parameters which define the non-linear mechanical behavior of human muscle tissue with the software package ABAQUS [11,12,13,10], with hyperelastic isotropic material model of Mooney – Rivlin. The strain energy function is defined by [9] as:

$$W = A_1(J_1 - 3) + A_2(J_2 - 3) + A_3(J_3^{-2} - 1) + A_4(J_3 - 1)^2, \quad (1)$$

Where J_1, J_2 and J_3 are the invariants of the right Cauchy-Green strain tensor. The right Cauchy-Green strain tensor is defined by [9]:

$$\boldsymbol{C} = \boldsymbol{F}^{\mathrm{T}} \cdot \boldsymbol{F}, \qquad (2)$$

where $\boldsymbol{F}$ is the deformation gradient tensor. The invariants J_1, J_2 and J_3 are defined [9] as:

$$\begin{aligned} J_1 &= trace(\boldsymbol{C}) \\ J_2 &= \frac{1}{2}\left(trace^2(\boldsymbol{C}) - trace(\boldsymbol{C})^2\right). \\ J_3 &= det(\boldsymbol{C}) \end{aligned} \qquad (3)$$

The second Piola-Kirchhoff stress tensor is obtained by differentiating the strain energy function W with respect to the right Cauchy-Green strain tensor [9]:

$$S = 2\frac{\partial W}{\partial C}.\qquad(4)$$

The material parameters A_3 and A_4 are function of the coefficients A_1 and A_2:

$$A_3 = \frac{1}{2}A_1 + A_2 \quad \text{and} \quad A_4 = \frac{A_1(5\nu - 2) + A_2(11\nu - 5)}{2(1 - 2\nu)}.\qquad(5)$$

The values for A_1, A_2 and ν have been set to: $A_1 = 0,00165$ MPa, $A_2 = 0,00335$ MPa and $\nu = 0,49$. These values for material parameters are used by Verver, M. [9].

The value for the density of human muscle tissue is defined with volume and body mass. The density of human muscle tissue is $0,0026$ kg/m^3.

4 Virtual model of driver's seat cushion with characteristics of the used materials

The driver's seat for passenger automobile consists mainly of three parts: seat cushion, seat back and head restraint. In Fig. 12, the seat cushion assembly is represented with the sheet metal holder and the polyurethane foam. The polyurethane foam from the seat cushion is placed on the sheet metal holder. The sheet metal is with thickness of 1 mm and is supported by the seat mechanical structure on four small perpendicular support areas.

Figure 12 Sheet metal holder, the foam from seat cushion

Figure 13 Virtual model of seat cushion

The driver's seat cushion for the driver's seat, shown in Fig. 12, is made by Johnson Controls. The geometrical

data are used for the analysis of the influence of the thickness and density of the polyurethane foam on the seating comfort.

The investigation begins with a virtual model of the seat cushion which is the same as the real seat, shown in Fig. 12. The virtual model of the seat cushion in Fig. 12 is shown in Fig. 13. In Fig. 13 we can see also two elliptical holes, which have a significant influence on the seat comfort. In Fig. 14, the dimensions of the seat cushion are shown.

The meshed model with tetrahedron elements is prepared to be used in FEA. The meshed model of the seat cushion, which corresponds to the virtual model of the seat in Fig. 13 is shown in Fig. 15.
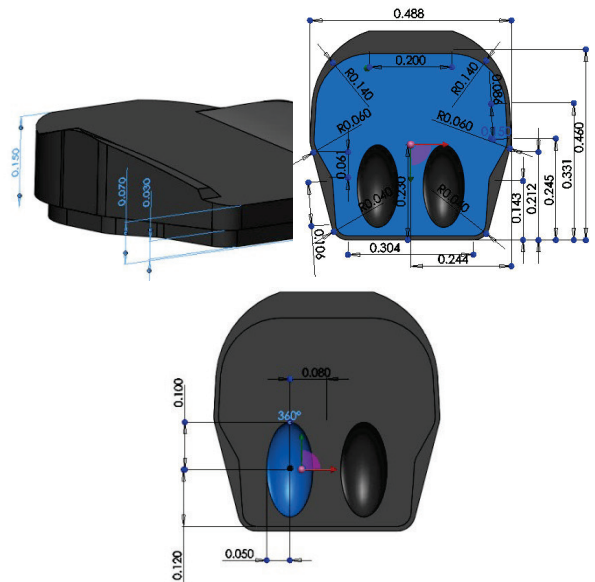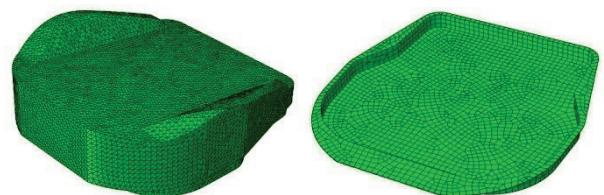

Figure 14 Dimensions of the seat cushion

Figure 15 The meshed model of seat cushion

As a means for the description of foam materials in ABAQUS [11, 12, 13, 10], a hyper-elastic law is used. The elasticity of the material is described via the potential energy U of elastic deformation. The applied potential function for foams (Eq. (6)) considers nearly full compressibility of polyurethane foams.

Strain energy potential of compressive foams is computed as Ogden function:

$$U = \sum_{i=1}^{N}\frac{2\mu_i}{\alpha_i^2}\left[\left(\lambda_1^{\alpha_i} + \lambda_2^{\alpha_i} + \lambda_3^{\alpha_i} - 3\right) + \frac{1}{\beta_i}\left(J^{-\alpha_i\beta_i} - 1\right)\right].\qquad(6)$$

The potential energy U is defined by the following parameters: μ_i are the coefficients of initial shear modulus, λ_{1-3} the principal stretches, α_i the standard material parameter, β_i the coefficients for degree of compressibility and J the elastic volume ratio. The free

material parameters μ_i, α_i and β_i are determined experimentally, with the average values out of loading and unloading.

With bold line in Fig. 16, are represented the nonlinear characteristics of polyurethane foam which is described with Ogden function with $N = 1$, $\mu = 10$ kPa, $\alpha = 8$ and Ogden function with $N = 2$, $\alpha_1 = 17,4$, $\mu_1 = 18,3$ kPa, $\alpha_2 = -2,0$, $\mu_2 = 0,21$ kPa and Poisson ratio $\nu = 0$ [14].
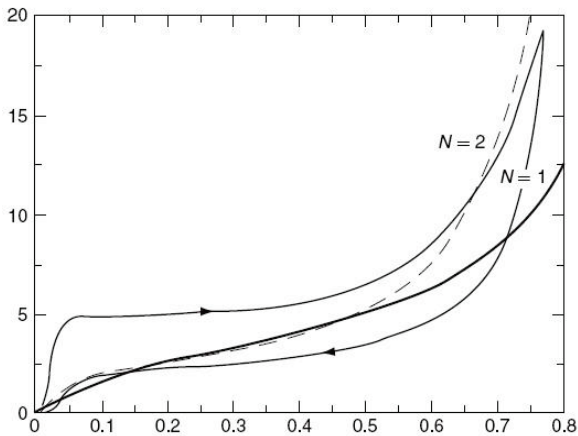

Figure 16 Nonlinear characteristic for flexible polyurethane foam [13]

Ogden function from second degree with $N = 2$ is used for description of nonlinear behavior of flexible polyurethane foam [10].

The density of polyurethane foam is given from the manufacturer Johnson Controls Inc. and is 50 kg/m^3.

5 Measurement equipment and testing of the model
5.1 Measurement equipment

For obtaining pressure distribution in the contact surface between the driver's seat and the driver the equipment from manufacturer XSENSOR Technology Corporation is used. The measurement equipment consists of a few elements such as: sensor platform X3 PRO, sensor pad for measuring of pressure distribution, Mini – B USB cable, 12 VDC 3.75 A AC/DC power supplier, electronic for connection of sensor pad and PC, X3 node, PC and software XSENSOR - X3 MEDICAL v6.0 used for data acquisition. The sensor pad is of type PX100:36.36.02 composed of a seat sensor with resolution of 1296 sensible points, with excellent flexibility and endurance. The measurement pressure range is between 10 ÷ 200 mmHg. The resolution of pressure measurement is 1,27 cm. The elements which are included in the measurement equipment for measuring of pressure distribution between two bodies in contact are shown in Fig. 17.

5.2 The results of experimental measuring and virtual testing

For measuring the pressure distribution between the driver's seat cushion from passenger automobile and the man, we use the seat described in Fig. 12. The measuring is performed with men from 50th and 80th percentile. The human weight of 50th percentile man before the testing

was 71 kg and for 80th percentile man was 78,5 kg. The measured weights are the same as the weights of the corresponding virtual models. Before the measuring the participants were seated according to the comfort angles. The measured pressure distribution and the values for maximum contact pressure are shown in Fig. 18.

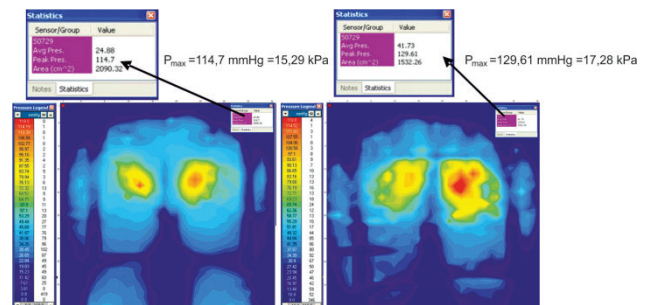**Figure 17** XSENSOR - X3 PRO system for measuring of pressure distribution

Figure 18 Pressure distributions between seat cushion and participants from 50th and 80th percentile

The boundary conditions in the simulation are defined on the seat geometry. In reality, the seat is fixed from below on four supports (in precisely defined areas) located on the sheet mental. The fixing is defined with translations and rotations equal to zero.

The initial conditions in the simulation are defined for the time $t = 0$ s. In the initial moment of the simulation, the virtual model of human is placed above the seat without a contact between them, and the initial speed is set to 0.

The loading condition in the simulation is defined with gravity of 9,81 m/s^2.

The contact between the virtual model of human and the seat cushion is defined with selecting of surfaces that come in contact. In reality, there is friction between contact surfaces. The coefficient of friction between contact surfaces is 0,75. The coefficient of friction is obtained experimentally [14].

The pressure distributions on the seat contact surface resulting from the analyses for 50th (left) and 80th (right) percentile are shown in Fig. 19.

The experimental values of the maximum contact pressure in the contact surface between the seat cushion

and the human are given in Tab. 2. The measured values are close to the values obtained from the virtual testing.
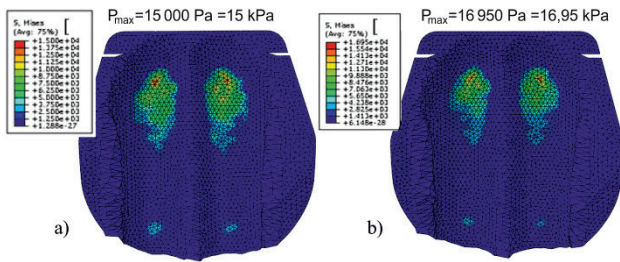

Figure 19 Pressure distributions on the contact surface of virtual seat cushion and virtual model of human from a) 50th and b) 80th percentile

Table 2 Values for maximum contact pressure

Human percentile	Maximum contact pressure from experimental measurement / kPa	Maximum contact pressure from virtual testing / kPa
50th percentile	15,29	15,00
80th percentile	17,28	16,95

The human skin and seat cover are not considered in the virtual testing. For this reason, there is a difference in the results obtained from the experiment and the virtual testing of about 2 %. This difference is small and approves the use of the virtual model instead of the experimental testing of seat prototypes.

6 Influence of thickness and density of polyurethane foam on the seating comfort

According to the data found in literature [14], comfortable seats are seats with maximum contact pressure less than 12 kPa.

For the seat geometry shown in Figs. 13 and 14, the influence of the foam thickness on the maximum contact pressure is examined using the virtual models of the seat and human from 50th and 80th percentile. The initial seat has foam thickness of 70 mm. If the foam thickness is reduced to 60 mm, 50 mm, and 40 mm, then the contact pressure increases, first slowly and then rapidly, such as shown in Fig. 20.
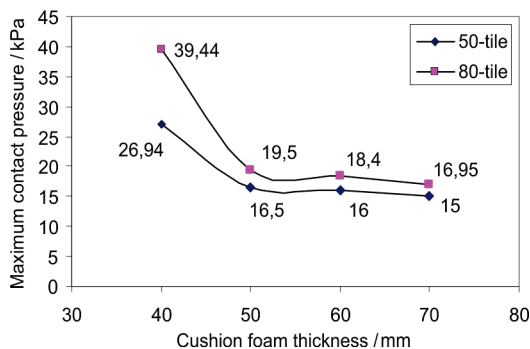

Figure 20 Relationship of maximum contact pressure and seat cushion thickness

To examine the influence of the density of the polyurethane foam on the contact pressure, six virtual testings for design shown in Figs. 13 and 14 are performed with the foam thickness of 70 mm. The results obtained from virtual testing of six virtual models of seats with density of 30 kg/m³, 40 kg/m³ and 50 kg/m³ and two

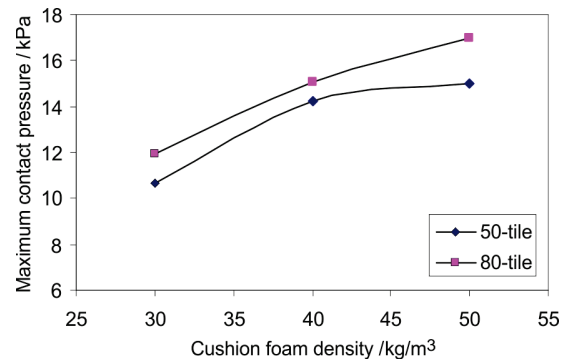types of virtual models of human from 50th and 80th percentile are shown in Fig. 21.

Figure 21 Relationship of maximum contact pressure and density of the polyurethane foam

7 Influence of contact seat surface shape on seating comfort

With changing of the seat design pressure, distribution map and value of maximum contact pressure also are changing. In Fig. 22 a car seat is shown which has the same dimensions as the seat shown in Fig. 13, with correction in the upper contact surface of the seat. On the upper seat surface which is in contact with the virtual model of human, more material from polyurethane foam is added. For seat design shown in Fig. 22 four virtual testings are made, with different densities of the polyurethane foam of 30 kg/m³ and 50 kg/m³ and with 50th and 80th percentile of mannequin.
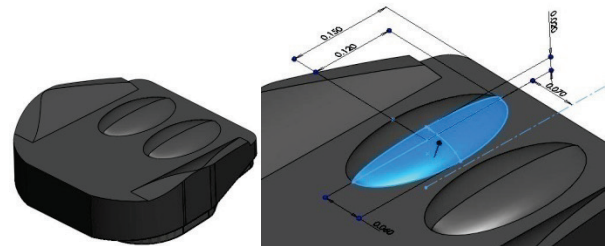

Figure 22 Virtual model of a new seat cushion

Maximum contact pressure between virtual model of the seat and virtual model of the human is read from pressure distribution map. In Tab. 3 a preview is given of obtained results with the change of the upper contact surface of the seat.

Tab. 3 shows that for lower density of polyurethane foam are obtained lower maximum pressures of contact surface of seat. It can also be concluded that lower density of polyurethane foam results in greater difference in maximum pressures for 50th percentile and 80th percentile of human.

Table 3 Maximum contact pressure for virtual model of seat shown in Fig. 22

Human percentile	Virtual model of seat with density of polyurethane foam of:	
	30 kg/m³	50 kg/m³
50th percentile	5,05 kPa	7,85 kPa
80th percentile	8,43 kPa	10,83 kPa

Big difference in results can be seen when the values of maximum contact pressure from Tab. 3 are compared. So, with adding of material on the upper surface of the seat, as shown in Fig. 22, the value of maximum pressure is reduced by about 50 %. The design has a significant impact on pressure distribution map and value of maximum contact pressure.

8 Conclusions

The virtual testing of seating process in driver's seat for passenger automobile allows fast and simplified review of the phenomena that occur during the seating. This virtual testbench provides a mechanism for investigation of new design ideas for new types of seats. Using this virtual testbench, the new design of seat can be validated in the product development phase, thus avoiding the financial costs and saving time for making physical prototypes.

The influence of the thickness of the seat cushion foam on the maximum contact pressure is examined. From the diagram shown in Fig. 20, it is obvious that with reducing the foam thickness below a certain limit value, the seating comfort is deteriorating gradually.

The foam density has an important influence on the value of the maximum contact pressure. As shown in Fig. 21, with reducing the foam density the value of the maximum contact pressure is decreasing slowly, and with that the seating comfort is improving.

The design has a significant impact on pressure distribution map and value of maximum contact pressure. With local adding of material corresponding to seat design, shown in Fig. 22, we can greatly affect the value of maximum contact pressure between virtual models of seat and human in order to improve seating comfort.

9 References

[1] Attwood, D. A.; Deeb, J. M.; Danz-Reece, M. E. Ergonomic Solutions for the Process Industries. Elsevier Inc, 2004.

[2] Kroemer, K. H. E. Extra – ordinary. // Ergonomics. Vol. 1, Taylor and Francis, 2006.

[3] Bernaer, J. D. Ergonomic for beginners, Second Edition, Taylor and Francis, 2001.

[4] CATIA V5 Tutorial, SIMULTIA Inc, 2008.

[5] Dickson, S. CATIA V5 Design with Analysis, The Hong Kong Polytechnic University, 2007.

[6] Karam, F.; Kleismit, C. CATIA V5.SDC Publications, 2006.

[7] Ebe, K.; Griffin, J. M. Factors affecting static seat cushion comfort, Taylor and Francis, 2001.

[8] Siefert, A.; Pankoke, S.; Wolfel, H. P. Virtual optimization of car passenger seats: Simulation of static and dynamic effects on driver' seating comfort. // International Journal of Industrial Ergonomics, Science Direct, 38, (2008), pp. 410-424.

[9] Verver, M. M. Numerical tools for comfort analysis of automotive seating. Dissertation, Technische Universiteit Eindhoven, 2004.

[10] Spyrakos, C. C.; Raftoyiannis, J. Linear and Nonlinear Finite Element Analysis In Engineering Practice. Algor Inc., 1997.

[11] ABAQUS Example Problems Manual. ABAQUS Inc., 2008.

[12] Getting Started with ABAQUS/Standard. ABAQUSInc., 2008.

[13] Liu, G. R.; Quek, S. S. The Finite Element Method: A Practical Course with Abaqus. Department of Mechanical Engineering, National University of Singapore, 2003.

[14] Nigel, J. M. Polymer Foams Handbook: Engineering and Biomechanics Applications and Design Guide. Butterworth - Heinemann, 2007.

Authors' addresses

Ile Mircheski, Ph-D, Assistant
Cyrill & Methodius University
Faculty of Mechanical Engineering
Karpos II - bb, 1000 Skopje
Republic of Macedonia
E-mail: ile.mircheski@mf.edu.mk
Phone: +389 2 3099 245

Tatjana Kandikjan, Ph-D, Full professor
Cyrill & Methodius University
Faculty of Mechanical Engineering
Karpos II - bb, 1000 Skopje
Republic of Macedonia
E-mail: tatjana.kandikjan@mf.edu.mk
Phone: +389 2 3099 256

Sofija Sidorenko, Ph-D, Full professor
Cyrill & Methodius University
Faculty of Mechanical Engineering
Karpos II - bb, 1000 Skopje
Republic of Macedonia
E-mail: sofija.sidorenko@mf.edu.mk
Phone: +389 2 3099 261